Paredes, Ferran; Herrojo, Cristian; Escudé Pujol, Roger; [et al.]. «High data density near-field chipless-RFID tags with synchronous reading». IEEE journal of radio frequency identification, Vol. 4, Issue 4 (December 2020), p. 517-524. DOI 10.1109/JRFID.2020.2996586

High Data Density Near-Field Chipless-RFID Tags with Synchronous Reading

Ferran Paredes, *Member, IEEE*, Cristian Herrojo, *Member, IEEE*, Roger Escudé, Eloi Ramon, and Ferran Martín, *Fellow, IEEE*

***Abstract*— Near-field chipless-RFID tags with high data density and synchronous reading capability are presented and experimentally validated in this paper. The tags consist of a chain of rectangular patches etched or printed at predefined positions on a dielectric substrate, including rigid or flexible (i.e., plastic or even paper) substrates. Patch dimensions determine the binary state, where the larger and smaller patches are associated with the logic '1' and '0' states, respectively, or vice versa. For sequentially and synchronously reading the bits, a sensitive element able to determine the presence of the patches and their size by proximity (through near field using microwaves) is considered. Such element is a microstrip line loaded with a pair of rectangular complementary split ring resonators (CSRRs), one etched inside the other in the ground plane. When the tag chain is displaced at short distance over the CSRRs, the larger patches modify the resonance frequency of both sensing CSRRs, whereas the lower patches do only alter the resonance frequency of the smaller CSRR. Consequently, the ID code is contained in the patch dimensions, and the presence of a patch (regardless of its size) determines the reading times (clock signal), necessary for synchronous reading. Tag reading in this system proceeds by feeding the CSRR-loaded line (reader) with a pair of harmonic signals tuned to the resonance frequencies of the bare CSRRs. Both signals are amplitude modulated (AM) at the output port as consequence of tag motion, and the respective envelope functions contain both the clock signal and the tag ID code. The ID codes of several 16-bit tags, implemented on different substrates (microwave substrate, plastic and paper) and exhibiting a per unit length density of 1.67 bit/cm, have been inferred with the dedicated reader for validation purposes.**

***Index Terms* — Chipless-RFID, synchronous reading, microwave encoders, microstrip technology.**

I. Introduction

CHIPLESS-RFID emerged more than one decade ago as an alternative to chip-based RFID, in order to reduce the cost of the tags (mainly dictated by the presence of the chip [1]). In most chipless-RFID systems, the identification (ID) code of the tags is contained in a metallic pattern, etched or printed on a dielectric substrate (rigid or flexible, including plastic and paper substrates). There are different encoding techniques in chipless-RFID, but the most extended one exploits the frequency domain [1]-[19]. In frequency-domain chipless-RFID systems, the tags contain resonant elements tuned to different frequencies, and the presence or absence of functional resonant elements determine the logic state ('1' or '0') of the corresponding resonator. It has been demonstrated that the data density and capacity of frequency-domain tags (or spectral signature barcodes, the usual designation of such tags) can be substantially enhanced by combining the frequency domain with other domains, e.g., phase, amplitude, polarization, etc. [20]-[33]. Nevertheless, the data capacity of these hybrid chipless-RFID systems is still far from the data storage capacity of chipped-tags (typically 96 bits according to the EPC UHF Gen2 standard).

Time-domain chipless-RFID systems based on tags emulating the behavior of surface acoustic wave (SAW) based tags [34] have been proposed. The working principle of such time-domain based tags is time-domain reflectometry (TDR), where the ID code is inferred from the echoes generated by a delay line loaded with reflectors in response to a pulsed interrogation signal. Several examples of TDR-based tags have been reported [35]-[44], but the data density and capacity of these tags is very limited as compared to the one of chip-based tags or SAW tags (the latter very competitive in terms of data capacity, but expensive, as far as they need acoustic transducers).

Recently, a novel time-domain approach for chipless-RFID systems, based on near-field coupling and sequential bit reading, has been reported by some the authors [45]-[56]. In these systems, the tags are implemented by etching or printing a chain of metallic inclusions (typically, although not exclusively, resonant elements) on a dielectric substrate (rigid or flexible, including plastic or paper). Encoding is based on the presence/absence of a functional inclusion at its predefined position in the tag chain, where each inclusion corresponds to a bit of information. For tag reading, the tag (i.e., the inclusions chain) is displaced at short distance over the sensitive part of the reader, an element able to discriminate between the functional and inoperative inclusions. The sensitive part of the reader is typically a transmission line, eventually loaded with a resonant element, fed by a harmonic signal conveniently tuned.

In contrast to frequency-domain or hybrid chipless-RFID systems, where the interrogation signal is a wideband signal, in these novel time-domain systems, a single-tone (harmonic) signal suffices for tag reading (two harmonic signals are needed for synchronous reading, as it will be shown later). Moreover, since the bits are read sequentially, the number of bits of the tags is theoretically unlimited (in practice the

This work was supported by MINECO-Spain (project TEC2016-75650-R), MICIU (project RTI2018-102070-B-C21), by *Generalitat de Catalunya* (project 2017SGR-1159), by *Institució Catalana de Recerca i Estudis Avançats* (who awarded Ferran Martín), and by FEDER funds.

F. Paredes, C. Herrojo, and F. Martín are with GEMMA/CIMITEC, Departament d'Enginyeria Electrònica, Universitat Autònoma de Barcelona, 08193 Bellaterra, Spain. E-mail: Ferran.Martin@uab.es.

R. Escudé, and E. Ramon are with Institut de Microelectronica de Barcelona IMB-CNM (CSIC), 08193 Bellaterra, Spain.

limitation is dictated by tag size). The sketch of the working principle (including synchronous reading) is depicted in Fig. 1. Note that the ID code is contained in the envelope function at the output port, with peaks or dips corresponding to the logic state '1' or '0', or vice versa.

The difference between these time-domain near-field chipless-RFID systems and the frequency-domain, or hybrid, systems mentioned above concerns the different type of ID data multiplexing. In frequency-domain and hybrid systems the data are multiplexed in frequency (the resonators are tuned to different frequencies), whereas in near-field chipless-RFID systems with sequential bit reading, the ID code is read bit by bit at different times, in a time-division multiplexing scheme. By analogy to the spectral signature barcodes (the usual designation of frequency-domain based tags), the tags in this novel time-domain and near-field approach of chipless-RFID have been called time-domain signature barcodes [52],[56].

For reading these time-domain signature barcodes, a mechanical guiding system able to displace at short distance, and with proper alignment, the linear inclusions' chain of the tag over the reader, is needed. Moreover, a constant relative velocity between the tag and the reader is required in order to avoid false readings. If such velocity is not known, but it is constant, the tags can be equipped with header bits in order to determine such velocity, and consequently the instants of time for bit reading [50]-[52]. Nevertheless, in order to provide major levels of robustness to the system, synchronous reading is very convenient (Fig. 1).

The main advantage of a synchronous system (a preliminary version was reported in [57]) is the fact that the displacement velocity of the tag does not need to be constant (as it may occur in a real scenario). This paper, an extension of the work presented in [57], reports a synchronous near-field chipless-RFID system where the inclusion's size in the direction of the chain axis are small, thereby reducing substantially the period of the inclusions. The result is a tag with high data density per unit length, the main figure of merit of this type of chipless-RFID tags. In [57], the reported prototype tags were implemented on a rigid microwave substrate. In this paper, the functionality of the system is demonstrated by reading the new designed tags by considering its implementation not only on microwave substrates, but also on plastic and paper substrates.

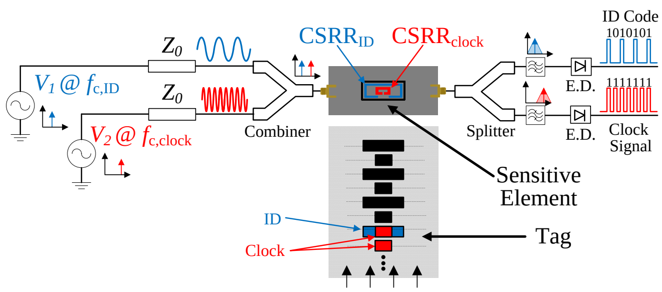

Fig. 1. Sketch of the time-domain near-field chipless-RFID systems with sequential and synchronous bit reading, showing the working principle. Through tag motion over the reader, electromagnetic coupling between the transmission line and the inclusions of the tag arise, and the output signals (for the ID code and clock) are amplitude modulated.

II. The Proposed Reader and Tags

The proposed near-field chipless-RFID system with synchronous reading capability is based on the approach first presented in [57]. The tags are implemented by means of a linear chain of rectangular patches, where each patch corresponds to a bit and encoding is achieved by patch size. Namely, patch dimensions determine the logic state, '1' or '0', of the corresponding bit. With this encoding system, a sensitive element able to determine, through near field coupling, the presence of a patch on top of it and patch dimensions, suffices to obtain both the ID code of the tag and the clock signal necessary for synchronous reading. Such sensitive element can be implemented by means of a microstrip transmission line loaded with a pair of complementary split ring resonators (CSRRs). It is well known that CSRR-loaded lines exhibit a transmission zero [58], which is intimately related to CSRR dimensions (and, obviously, to the characteristics of the considered substrate, mainly thickness and dielectric constant). However, the presence of a metal patch in close proximity to it also modifies the position of the transmission zero frequency, provided the patch boundaries extend beyond the perimeter of the CSRR.

According to the previous works, the presence of a patch in the tag chain and its size can be inferred by considering two CSRR, one inside the other one, rather than one. The specific topology of the reader CSRR-loaded line is depicted in Fig. 2(a), whereas Fig. 2(b) shows the layout of the tag, with the presence of both binary states (larger and smaller patches). Note that the CSRRs are single loop slot resonators with the slits etched at the same position. This is important, in order to avoid inter-slot coupling [59]. Therefore, with this pattern in the ground plane, the two CSRRs behave as individual, roughly uncoupled, resonators. A slot ring surrounds the outer CSRR in order to tailor its quality factor.

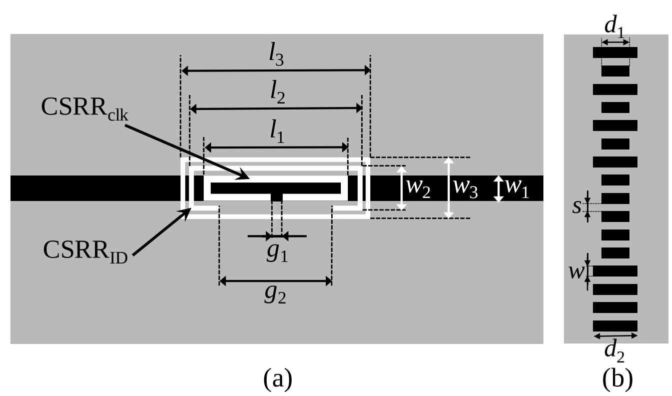

Fig. 2. Topology of the proposed reader (a) and tag (b). The considered substrate for the reader is the *Rogers RO4003C* with dielectric constant $\varepsilon_r = 3.38$, thickness h = 0.81 mm and loss factor $\tan\delta = 0.0022$. Relevant reader dimensions are: l_1 = 10.3 mm; l_2 = 12.3 mm, l_3 = 13.5 mm, w_1 = 1.9 mm, w_2 = 3.1 mm, w_3 = 4.3 mm, g_1 = 1.0 mm, g_2 = 7.2 mm. CSRR slots width are c_1 = 0.5 mm and c_2 = 0.3 mm for the inner and the outer CSRR, respectively, and the outer slot ring width is c = 0.3 mm. The considered microwave substrate for one of the fabricated tags is the *Rogers RO4003C* with dielectric constant $\varepsilon_r = 3.38$, thickness h = 0.2 mm and loss factor $\tan\delta = 0.0022$. Tag dimensions are: d_1 = 9.3 mm; d_2 = 14.5 mm, s = 3 mm and w = 3 mm.

The functionality of the system proceeds as follows. Regardless of its size, a patch on top of both resonators is able to modify the resonance frequency of the smaller CSRR. However, the external CSRR is only altered by the larger patches. Consequently, the larger CSRR is used to discriminate the binary state, whereas the inner CSRR is devoted to generate the synchronization clock signal. For that purpose, two harmonic signals tuned to the resonance frequencies of the bare resonators (designated as $f_{c,ID}$ and $f_{c,clock}$) must be injected to the input port of the CSRR-loaded line. It is expected that the presence of any patch modifies the resonance of the inner CSRR, generating a large excursion of the transmission coefficient at $f_{c,clock}$, and thereby producing a significant variation (increment) of the amplitude of the harmonic signal tuned to that frequency. Thus, the clock signal is merely the envelope function of the amplitude modulated (AM) signal with carrier frequency $f_{c,clock}$, with as many peaks as patches in the tag chain. Conversely, for the envelope function of the output AM signal with carrier frequency tuned to $f_{c,ID}$, it is expected that peaks appear only at those clock instants where the patches on top of the CSRRs are those with larger dimensions.

Figure 3 depicts the frequency response of the CSRR-loaded reader line without patch loading, as well as the responses with larger and smaller patch on top of the CSRRs. The considered air gap (distance between the patch and CSRRs) is 0.5 mm. As it can be appreciated, the notch frequencies vary in agreement to the predictions of the precedent paragraph. Moreover, a significant excursion of the transmission coefficient at both frequencies, $f_{c,clock}$ and $f_{c,ID}$, when the patch is able to shift the corresponding frequency, can be seen. This is important in order to obtain a high modulation index of both AM signals at the output port, a key aspect in terms of system robustness, to clearly discriminate between the two binary states.

To gain further insight on the functionality of the proposed system, Fig. 4 depicts the variation of the transmission coefficient at $f_{c,clock}$ and $f_{c,ID}$, as the tag with the indicated code is displaced over the CSRR of the reader. The peaks at periodic positions of the clock curve indicate the presence of a patch on top of the CSRR, whereas for the ID curve, the peaks correlate with the presence of a larger patch above the position of the CSRRs (logic state '1').

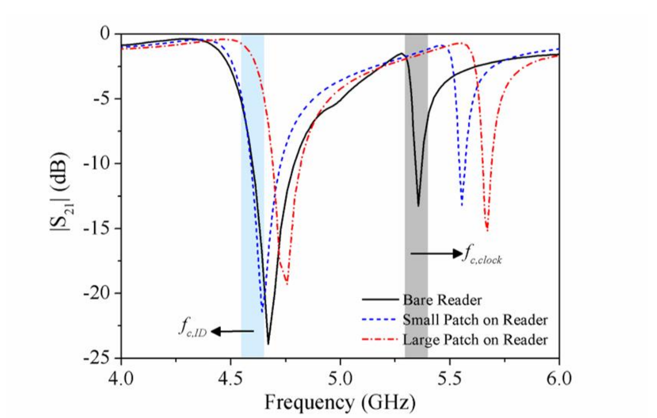

Fig. 3. Simulated frequency response (transmission coefficient) of the bare reader and reader loaded with smaller and larger patch. The simulation has been carried out by means of the *Keysight Momentum* software.

III. Experimental validation of tag reading

The photograph of the fabricated CSRR-loaded reader line is depicted in Fig. 5 (the considered substrate is indicated in the caption of Fig. 2). Concerning the tag, we have considered as first option the fabrication on a microwave substrate, particularly, the *Rogers RO4003C* with dielectric constant ε_r = 3.38, thickness h = 0.2 mm and loss factor tanδ = 0.0022. Nevertheless, since the tag reading scheme is based on the variation of the transmission coefficient generated by the metallic patches of the tags, it is expected that the influence of the tag substrate on system functionality is not critical. Consequently, we have also fabricated tags on flexible substrate, including plastic substrate (*Polyethylene naphthalate*, or also known as *PEN*, with a thickness h = 125 μm, from *Dupont*) and paper (*Powercoat XD* with a thickness h = 200 μm, from *Arjowinngs*), in both cases by means of inkjet printing (details of the inkjet printing

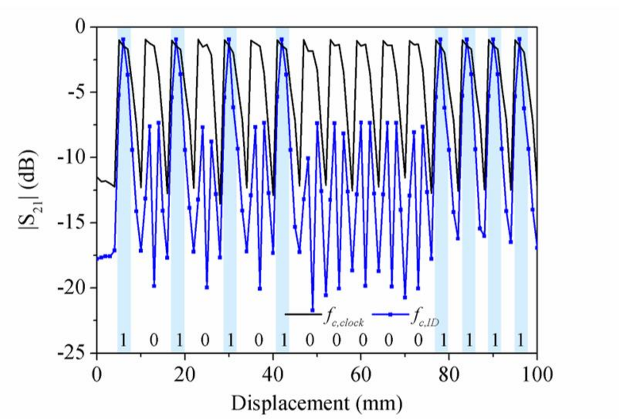

Fig. 4. Simulated transmission coefficient at $f_{c,clock}$ and $f_{c,ID}$, as the tag with the indicated code is displaced over the CSRR of the reader. The simulation has been carried out by means of the *Keysight Momentum* software.

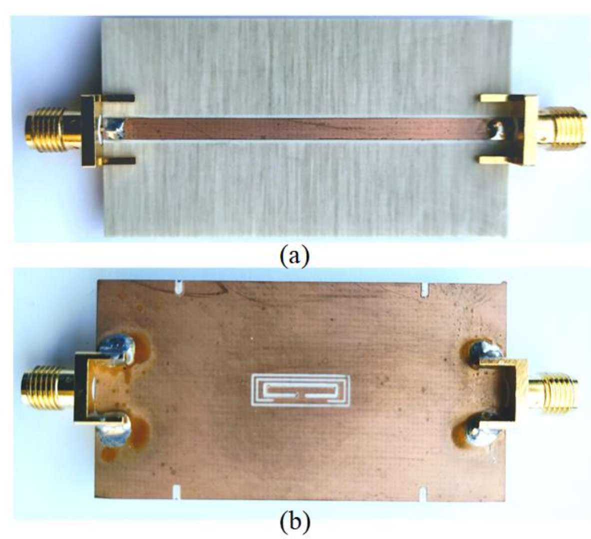

Fig. 5. Photograph of the sensitive part of the reader. (a) Top; (b) bottom.

process are given in [50]-[52]) and by using the *Orgacon Nanosilver* Inkjet Ink from the *AGFA*. The fabricated prototypes are shown in Fig. 6.

For validation purposes, we have generated the interrogation harmonic signals (tuned to $f_{c,clock}$ = 5.31 GHz and $f_{c,ID}$ = 4.63 GHz) by means of the function generator *Agilent E4438C*. In order to obtain the envelope function, an AM detector based on the *Avago HSMS-2860* Schottky diode and the *Agilent N2795A* active probe (with resistance and capacitance R = 1 MΩ and C = 1 pF, respectively) has been implemented. Moreover, the *ATM PNR ATc4-8* circulator, configured as an isolator, has been cascaded between the output port of the reader line and the AM detector in order to prevent from unwanted reflections from the diode. The envelope signals corresponding to the clock signal and ID code have been visualized on an oscilloscope (model *Agilent MSO-X 3104A*). Finally, tag displacement over the reader line has been carried out by means of a linear stepper motor (model *THORLABS LTS300/M*). The photograph of the complete experimental setup is depicted in Fig. 7.

It should be mentioned that in a real scenario, either a combiner/diplexer (see Fig. 1) or a switching scheme is needed in order to separately obtain the envelope functions of the clock signal and ID code. The schematic of the system by considering the switching scheme, the most convenient in terms of space and cost, is depicted in Fig. 8. Nevertheless, system validation in this paper is done by independently injecting the harmonic signals to the input port of the reader line and inferring the corresponding envelope function. The results for the different considered tags are shown next.

The envelope functions of the different measured tags (see Fig. 6), including the clock signals and the ID code signals, are depicted in Fig. 9. It can be seen in this figure that the peaks in the ID signals perfectly correlate with the logic state '1' of the corresponding ID code (larger patches), as expected, and as many peaks as number of bits (or patches) in the clock signal are present. Therefore, these results validate the proposed near-field chipless-RFID approach with synchronous reading. It is important to highlight that the system is functional even by considering the implementation of inkjet-printed tags on paper, representing an excellent solution in terms of tag cost.

Concerning tag dimensions, an important aspect to emphasize is the fact that for synchronous reading, an additional chain of inclusions is not needed (this is obviously the most trivial solution, but it requires not only an additional chain, but also a more complex sensing element for the reader, with at least two separately allocated resonant elements). With the proposed reader, based on a pair of rectangular-shaped

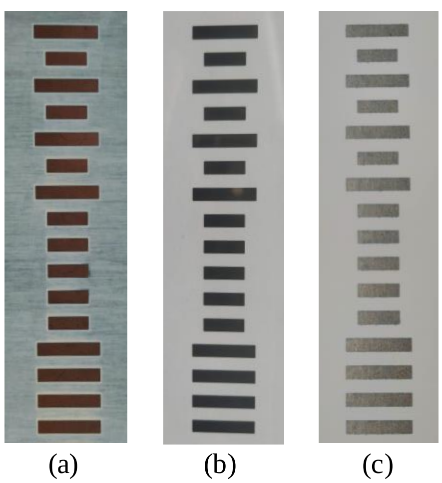

Fig. 6. Photograph of the fabricated tags on microwave substrate (a), plastic substrate (b) and paper (c).

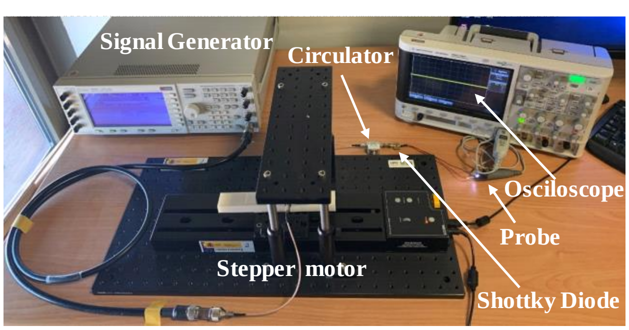

Fig. 7. Experimental setup used for tag reading.

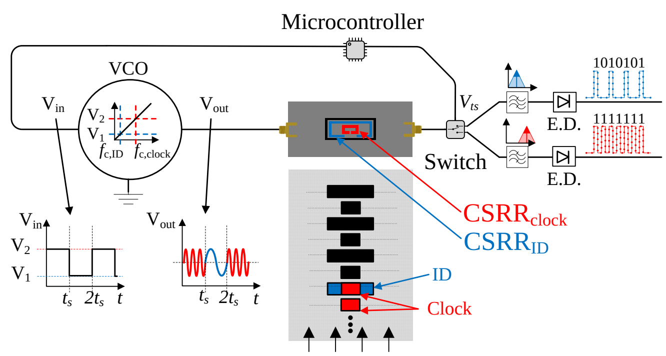

Fig. 8. Sketch of the near-field chipless-RFID system with synchronous reading capability based on a switching scheme.

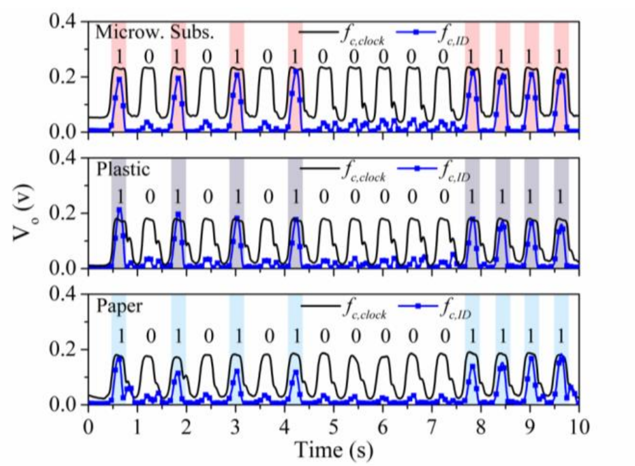

Fig. 9. Clock and ID signals inferred by reading the fabricated tags in microwave substrate, in plastic substrate and in ordinary paper, respectively, with the experimental setup of Fig. 7.

CSRRs one inside the other, the period of the inclusions is of 6 mm. This represents an important improvement in terms of data density per unit length (DPL), as compared to the first implementation of the approach, reported in [57]. For the tags of Fig. 6, such density is DPL = 1.67 bit/cm, whereas in [57] the result is DPL = 0.67 bit/cm. Despite the fact the main figure of merit of these tags based on linear chains of inclusions is the DPL (it must be as much as small as possible in order to avoid excessively lengthy tags), the density per surface (DPS) is very reasonable. By considering the minimum rectangle that contains the chain patches, the density per surface is found to be DPS = 1.15 bit/cm^2. These values of DPL and DPS are not as good as those, e.g., reported in [55], where chains based on closely spaced linear strip were considered. However, in [55], the tags do not exhibit synchronous reading capability.

Another important aspect of the proposed tags is their robustness against mechanical wearing. In the reported near-field chipless-RFID systems reported so far [45]-[55], where the metallic tag inclusions are either resonant elements or linear strips, an unexpected cut or crack in those tag inclusions may generate a bit error, as far as the inclusion losses its functionality. Indeed, deliberate resonator's cutting is a method for tag programming, or reprogramming, as discussed in [50]. However, the effects of a metallic patch on top of a CSRR (resonance shift) do not vanish if small-unexpected cuts or cracks (that may appear as consequence of mechanical wearing) are present. Obviously, this is not true if large cracks or a significant damage in the metal layer of the patch (e.g., caused by extreme friction) occur. To demonstrate this robustness of the proposed tags against wearing/friction, we have deliberately generated cuts in the fabricated tags. To do that, we have simply generated transverse cuts, as depicted in Fig. 10. The responses of these cracked tags are depicted in Fig. 11. According to the obtained responses, the periodic peaks in the clock signals are perfectly visible, and the ID code signal for each cracked tag perfectly provides the ID code. These results confirm the capability of the system to maintain the ID code despite the presence of cracks in the patches.

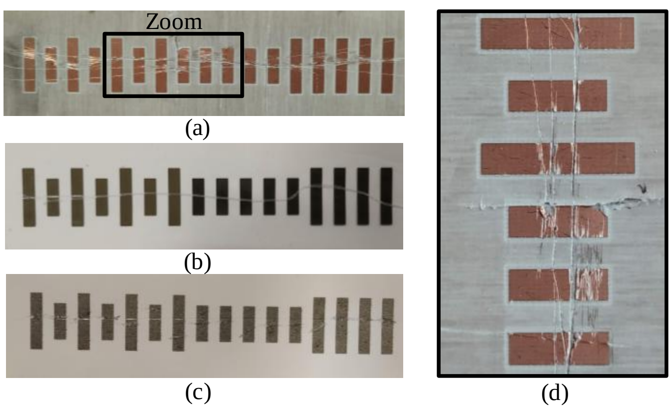

Fig. 10. Photograph of the cracked tags on microwave substrate (a), plastic substrate (b), paper (c), and zoom view of cracked patches of the microwave substrate (d).

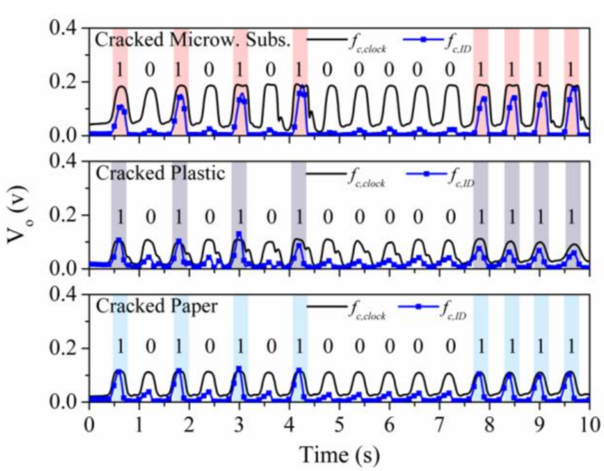

Fig. 11. Clock and ID signals inferred by reading a microwave substrate, plastic and paper-based tag with cracks in all patches.

IV. Discussion

One important aspect of this type of chipless-RFID systems is the tolerance against lateral misalignments and air gap variations between the tag and the reader, eventually caused by vibration, or by any other mechanical issue. An estimation of such tolerances can be inferred by repeating the simulations of Fig. 3, considering small lateral misalignments (Fig. 12) and variations in the air gap distance (Fig. 13), for the larger and smaller patches. These results demonstrate that, in the case of larger patches, lateral misalignments higher than 1 mm deteriorate the dynamic range of the lower frequency $f_{c,ID}$ (4.63 GHz), but they have no effect in the higher frequency $f_{c,clock}$ (5.31 GHz). On the other hand, the variation (excursion) between the curves for the bare reader and reader loaded with the smaller patches at higher frequencies is not very significant. However, at low frequencies, for misalignments higher than 1 mm, the smaller patch has influence on the external CSRR, and consequently, the dynamic range is considerably affected. This effect could be improved by shortening the smaller patches. Similarly, Fig. 13 indicates that the air gap can be expanded from 0.25 up to 0.75 mm (outside this range, it cannot be guaranteed that the patches are correctly detected).

Concerning the data density of the reported tags, it is better than the one of the tags of [57]. However, it is not as good as the one of previous tags based on a similar principle (but not including synchronous reading capability). Particularly, the tag density in papers [54] and [55] is very good (e.g., a DPL = 17.7 bit/cm and a DPS = 26.04 bit/cm^2 were obtained in [55], by virtue of the considered tag inclusions, i.e., narrow strips). The worst tag density of the proposed tags is compensated by synchronous reading, an advantageous aspect not reported in [54],[55], and necessary in certain applications where a constant and well known velocity between the tag and the reader cannot be guaranteed. Moreover, the tags of this paper are robust against potential effects caused by tag friction (eventually generating cracks in the tags), as demonstrated in Figs. 10 and 11.

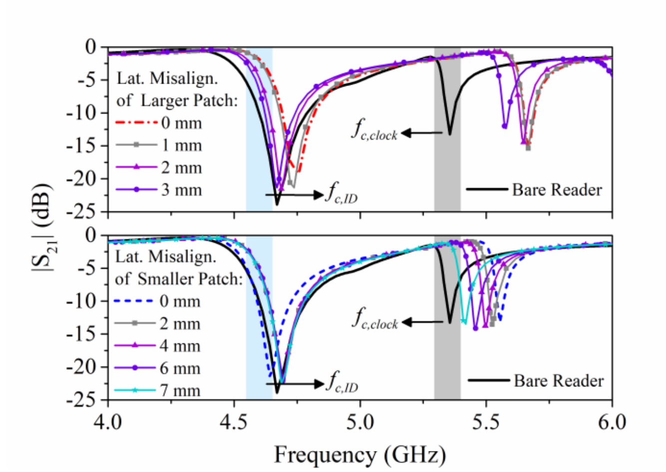

Fig. 12. Simulated frequency response (transmission coefficient) of the reader loaded with smaller and larger patch, by considering lateral misalignments. The simulations have been carried out by means of the *Keysight Momentum* software.

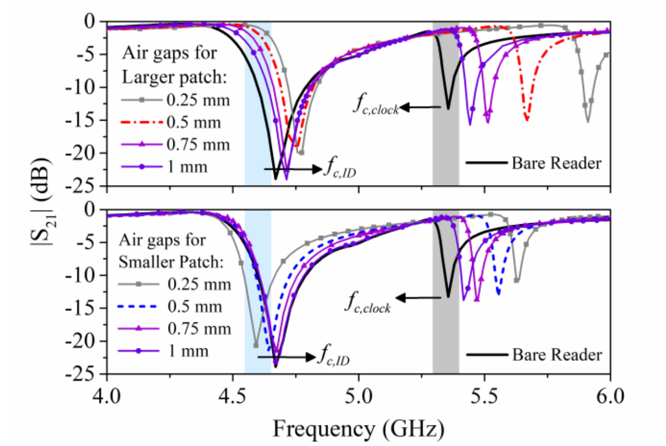

Fig. 13. Simulated frequency response (transmission coefficient) of the reader loaded with smaller and larger patch, by considering air gap variations. The simulations have been carried out by means of the *Keysight Momentum* software.

Finally, let us indicate that the reported reader/tag does not belong to the class of near-field RFID systems operating at 13.56 MHz and based on NFC between the tag and the reader by using inductive loops. However, tag reading proceeds by proximity (and alignment) in the proposed system. The tag patches perturb the electromagnetic field in the vicinity of the CSRRs, thereby modifying their resonance frequency. For this main reason, it is reasonable to designate these systems as near-field chipless RFID systems.

V. Conclusions

In conclusion, a near-field chipless-RFID system with synchronous reading has been presented and validated in this paper. The tags consist of a chain of metal patches etched or printed on a dielectric substrate, and tag encoding is achieved by patch size. The sensitive element of the reader is a microstrip line loaded with a pair of CSRRs. Such reader is able to detect the presence of a patch regardless of its size (through electromagnetic coupling between the patch and the smaller CSRR), thereby generating the clock signal necessary for synchronous bit reading. Additionally, the larger CSRR is only sensitive to the larger patches, this being the resonator devoted to determine the ID code of the tag. The system has been validated by means of a dedicated setup, which uses a step motor to displace the tag over the reader. Moreover, tag reading is based on an AM detector, necessary to provide the envelope function of the AM modulated clock and ID signals. System functionality has been demonstrated by considering tags implemented on microwave and flexible substrates, including paper, and it has been found that the tags are tolerant to the presence of cuts or cracks in the patches, which may be caused by wearing or friction in a real scenario. The key figures of merit in these near-field chipless-RFID tags based on linear chains of inclusions, the information density per unit length and the information density per surface, have been found to be very reasonable, i.e., DPL = 1.67 bit/cm and DPS = 1.15 bit/cm^2. This later value is high taking into account the synchronous reading capability of the system, and has been achieved by avoiding an extra chain for the generation of the clock signal. As compared to optical barcodes, the proposed tags are not as cheap and easy to read. However, the optical barcodes can be easily reproduced (by simply photocopying them), and the copy has exactly the same properties as the original. By contrast, with the proposed system, a copied tag cannot be read with the designed and fabricated ad hoc reader, unless a printing process (using conductive inks) makes the copy. This is the main advantage over optical barcodes, i.e., the proposed system provides certain level of security against plagiarism of coded documents, for instance, or other premium products.

References

[1] S. Preradovic and N. C. Karmakar, "Chipless RFID: bar code of the future," *IEEE Microwave Magazine*, vol. 11, pp. 87-97, 2010.
[2] S. Preradovic and N. C. Karmakar, Multiresonator-Based Chipless RFID: Barcode of the Future, Springer, 2011.
[3] I. Jalaly and I. D. Robertson, “RF barcodes using multiple frequency bands,” in *IEEE MTT-S International Microwave Symposium Digest*, Long Beach, USA, Jun. 2005, pp. 139–142.
[4] S. Preradovic, I. Balbin, N. C. Karmakar, and G. F. Swiegers, "Multiresonator-based chipless RFID system for low-cost item tracking," *IEEE Trans. Microw. Theory Techn.*, vol. 57, pp. 1411-1419, 2009.
[5] S. Preradovic and N. C. Karmakar, "Design of chipless RFID tag for operation on flexible laminates," *IEEE Anten. Wireless Propag. Lett.*, vol. 9, pp. 207-210, 2010.
[6] J. McVay, A. Hoorfar, and N. Engheta, “Space-filling curve RFID tags,” in Proc. of *2006 IEEE Radio Wireless Symp.*, pp. 199–202.
[7] I. Jalaly and D. Robertson, “Capacitively-tuned split microstrip resonators for RFID barcodes,” in Proc. of *European Microwave Conference*, October 2005, vol. 2, pp. 4–7.
[8] H.-S. Jang, W.-G. Lim, K.-S. Oh, S.-M. Moon, and J.-W. Yu, “Design of low-cost chipless system using printable chipless tag with electromagnetic code”, *IEEE Microw. Wireless Compon. Lett.*, vol. 20, pp. 640-642, 2010.
[9] A. Vena, E. Perret, and S. Tedjini, “A fully printable chipless RFID tag with detuning correction technique”, *IEEE Microw. Wireless Compon. Lett.*, vol. 22(4), pp. 209-211, 2012.
[10] A. Vena, E. Perret, and S. Tedjini, “Design of compact and auto-compensated single-layer chipless RFID tag”, *IEEE Trans. Microw. Theory Techn.*, vol. 60(9), pp. 2913-2924, Sep. 2012.
[11] A. Vena, E. Perret, and S. Tedjini, “High-capacity chipless RFID tag insensitive to the polarization”, *IEEE Trans. Ant. Propag.*, vol. 60(10), pp. 4509-4515, Oct. 2012.
[12] D. Girbau, J. Lorenzo, A. Lazaro, C. Ferrater, and R. Villarino, “Frequency-coded chipless RFID tag based on dual-band resonators,” *IEEE Ant. Wireless Propag. Lett.*, vol. 11, pp. 126–128, 2012.

[13] M. M. Khan, F. A. Tahir, M. F. Farooqui, A. Shamim, H. M. Cheema, "3.56-bits/cm^2 compact inkjet printed and application specific chipless RFID tag," *IEEE Ant. Wireless Propag. Lett*., vol. 15, pp. 1109-1112, 2016.

[14] R. Rezaiesarlak and M. Manteghi, "Complex-natural-resonance-based design of chipless RFID tag for high-density data," *IEEE Trans. Ant. Propag.*, vol. 62, pp. 898-904, Feb. 2014.

[15] M. S. Bhuiyan and N. Karmakar, "A spectrally efficient chipless RFID tag based on split-wheel resonator," in *Int. Antenna Technol. Workshop on Small Antennas, Novel EM Struct., Mater., Appl*., 2014, pp. 1–4.

[16] C. M. Nijas *et al*., "Low-cost multiple-bit encoded chipless RFID tag using stepped impedance resonator," *IEEE Trans. Ant. Propag*., vol. 62, no. 9, pp. 4762–4770, Sep. 2014.

[17] J. Machac and M. Polivka, "Influence of mutual coupling on performance of small scatterers for chipless RFID tags," in *24th Int. Radioelektron. Conf*., 2014, pp. 1–4.

[18] M. Svanda, J. Machac, M. Polivka, J. Havlicek., "A comparison of two ways to reducing the mutual coupling of chipless RFID tag scatterers," in Proc. of *21st International Conference on Microwave, Radar and Wireless Communications (MIKON)*, May 2016, pp. 1-4.

[19] C. Herrojo, J. Naqui, F. Paredes and F. Martín, "Spectral signature barcodes based on S-shaped Split ring resonators (S-SRR)", *EPJ Applied Metamaterials*, vol. 3, pp. 1-6, Jun. 2016.

[20] A. Vena, E. Perret, S. Tedjini, "Chipless RFID tag using hybrid coding technique," *IEEE Trans. Microw. Theory Techn.*, vol. 59, pp. 3356-3364, Dec. 2011.

[21] A. Vena, E. Perret, S. Tedjini, "A compact chipless RFID tag using polarization diversity for encoding and sensing", *2012 IEEE Int. Conf. RFID*, pp. 191-197, 2012.

[22] M. A. Islam and N. C. Karmakar, "A novel compact printable dual-polarized chipless RFID system," *IEEE Trans. Microw. Theory Techn.*, vol. 60, pp. 2142-2151, Jul. 2012.

[23] I. Balbin, N.C. Karmakar, "Phase-encoded chipless RFID transponder for large scale low cost applications", *IEEE Microw. Wireless. Compon. Lett.*, vol. 19, pp. 509-511, 2009.

[24] S. Genovesi, F. Costa, A. Monorchio, G. Manara, "Chipless RFID tag exploiting multifrequency delta-phase quantization encoding", *IEEE Ant. Wireless Propag. Lett.*, vol. 15, pp. 738-741, 2015.

[25] O. Rance, R. Siragusa, P. Lemaitre-Auger, and E. Perret, "RCS magnitude coding for chipless RFID based on depolarizing tag," in *IEEE MTT-S Int. Microw. Symp. Dig*., 2015, pp. 1–4.

[26] O. Rance, R. Siragusa, P. Lemaître-Auger, E. Perret, "Toward RCS magnitude level coding for chipless RFID," *IEEE Trans. Microw. Theory Techn.*, vol. 64, pp. 2315-2325, Jul. 2016.

[27] C. Herrojo, J. Naqui, F. Paredes, F. Martín, "Spectral signature barcodes implemented by multi-state multi-resonator circuits for chipless RFID tags", *IEEE MTT-S International Microwave Symposium* (IMS'16), San Francisco, May 2016.

[28] C. Herrojo, F. Paredes, J. Mata-Contreras, S. Zuffanelli and F. Martín, "Multi-state multi-resonator spectral signature barcodes implemented by means of S-shaped Split Ring Resonators (S-SRR)", *IEEE Trans. Microw. Theory Techn.*, vol. 65, no. 7, pp. 2341-2352, Jul. 2017.

[29] S. Gupta, B. Nikfal, and C. Caloz, "Chipless RFID system based on group delay engineered dispersive delay structures," *IEEE Ant. Wireless Propag. Lett*., vol. 10, pp. 1366–1368, 2011.

[30] R. Nair, E. Perret, and S. Tedjini, "Chipless RFID based on group delay encoding," in *IEEE Int. RFID-Technol. Appl. Conf*., 2011, pp. 214–218.

[31] C. Feng, W. Zhang, L. Li, L. Han, X. Chen, and R. Ma, "Angle-based chipless RFID tag With high capacity and insensitivity to polarization," *IEEE Trans. Ant. Propag*., vol. 63, no. 4, pp. 1789–1797, Apr. 2015.

[32] A. El-Awamry, M. Khaliel, A. Fawky, M. El-Hadidy, and T. Kaiser, "Novel notch modulation algorithm for enhancing the chipless RFID tags coding capacity," in *IEEE Int. RFID Conf*., 2015, pp. 25–31.

[33] A. Vena, A. A. Babar, L. Sydanheimo, M. M. Tentzeris, and L. Ukkonen, "A novel near-transparent ASK-reconfigurable inkjet-printed chipless RFID tag," *IEEE Ant. Wireless Propag. Lett*., vol. 12, pp. 753–756, 2013.

[34] C. S. Hartmann, "A global SAW ID tag with large data capacity," in Proc. of *IEEE Ultrasonics Symposium*, October 2002, vol. 1, pp. 65–69.

[35] A. Chamarti and K. Varahramyan, "Transmission delay line based ID generation circuit for RFID applications," *IEEE Microw. Wireless Compon. Lett.*, vol. 16, pp. 588-590, 2006.

[36] M. Schüßler, C. Damm, and R. Jakoby, "Periodically LC loaded lines for RFID backscatter applications," in Proc. of *Metamaterials 2007*, Rome, Italy, October 2007, pp. 103-106.

[37] M. Schüßler, C. Damm, M. Maasch, and R. Jakoby, "Performance evaluation of left-handed delay lines for RFID backscatter applications," in Proc. of the *IEEE MTT-S International Microwave Symposium 2008*, pp. 177-180.

[38] B. Shao, Q. Chen, Y. Amin, D. S. Mendoza, R. Liu, and L.-R. Zheng, "An ultra-low-cost RFID tag with 1.67 Gbps data rate by ink-jet printing on paper substrate," in *IEEE Asian Solid State-Circuits Conf*., 2010, pp. 1–4.

[39] F.J. Herraiz-Martínez, F. Paredes, G. Zamora, F. Martín, and J. Bonache, "Printed magnetoinductive-wave (MIW) delay lines for chipless RFID applications", *IEEE Trans. Ant. Propag*., vol. 60, pp. 5075-5082, Nov. 2012.

[40] S. Tedjini, E. Perret, A. Vena, D. Kaddout, "Mastering the electromagnetic signature of chipless RFID tags", in *Chipless and Conventional Radiofrequency Identification*, ed. IGI Global, 2012.

[41] L. Zhang, S. Rodriguez, H. Tenhunen, and L.-R. Zheng, "An innovative fully printable RFID technology based on high speed time-domain reflections," in *Conference on High Density Microsystem Design and Packaging and Component Failure Analysis, 2006.* HDP'06., Shanghai, China, Jun. 2006, pp. 166–170.

[42] L. Zheng, S. Rodriguez, L. Zhang, B. Shao, and L.-R. Zheng, "Design and implementation of a fully reconfigurable chipless RFID tag using Inkjet printing technology," in *2008 IEEE International Symposium on Circuits and Systems*, Seattle, USA, May 2008, pp. 1524–1527.

[43] C. Mandel, M. Schussler, M. Maasch, and R. Jakoby, "A novel passive phase modulator based on LH delay lines for chipless microwave RFID applications," in 2009 *IEEE MTT-S International Microwave Workshop on Wireless Sensing, Local Positioning, and RFID*, Cavtat, Croatia, Sep. 2009, pp. 1–4.

[44] R. Nair, E. Perret, and S. Tedjini, "Temporal multi-frequency encoding technique for chipless RFID applications," in *IEEE MTT-S International Microwave Symposium Digest*, Montreal, Canada, Jun. 2012, pp. 1–3.

[45] C. Herrojo, J. Mata-Contreras, F. Paredes, Ferran Martín, "Near-field chipless RFID encoders with sequential bit reading and high data capacity", *IEEE MTT-S Int. Microw. Symp.* (IMS'17), Honolulu, Hawaii, June 2017.

[46] C. Herrojo, J. Mata-Contreras, F. Paredes, F. Martín, "Microwave encoders for chipless RFID and angular velocity sensors based on S-shaped split ring resonators (S-SRRs)", *IEEE Sensors J.*, vol. 17, pp. 4805-4813, Aug. 2017.

[47] C. Herrojo, J. Mata-Contreras, F. Paredes, A. Núñez, E. Ramón, F. Martín, "Near-field chipless-RFID tags with sequential bit reading implemented in plastic substrates", *Int. J. Magnetism. Magnetic Mat*., published online, https://doi.org/10.1016/j.jmmm.2017.10.005.

[48] C. Herrojo, J. Mata-Contreras, F. Paredes, F. Martín, "High data density and capacity in chipless radiofrequency identification (chipless-RFID) tags based on double-chains of S-shaped split ring resonators (S-SRRs)", *EPJ Appl. Metamat.*, vol. 4, article 8, 6 pages, Oct. 2017.

[49] C. Herrojo, J. Mata-Contreras, F. Paredes, Ferran Martín, "Near-field chipless RFID system with high data capacity for security and authentication applications", *IEEE Trans. Microw. Theory Techn*., vol. 65 (12), pp. 5298-5308, Dec. 2017.

[50] C. Herrojo, J. Mata-Contreras, F. Paredes, A. Núñez, E. Ramon, and F. Martín "Near-field chipless-RFID system with erasable/programmable 40-bit tags inkjet printed on paper substrates", *IEEE Microw. Wireless Compon. Lett.*, vol. 28, pp. 272- 274, Mar. 2018.

[51] C. Herrojo, J. Mata-Contreras, F. Paredes, A. Núñez, E. Ramon, and F. Martín, "Very Low-Cost 80-Bit Chipless-RFID Tags Inkjet Printed on Ordinary Paper," *Technologies*, vol. 6, no. 2, p. 52, May 2018.

[52] C. Herrojo, F. Paredes, J. Mata-Contreras, E. Ramon, A. Núñez, F. Martín, "Time-domain signature barcodes: near-field chipless-RFID systems with high data capacity", *IEEE Microwave Magazine*, vol. 20, no. 12, pp. 87-101, Dec. 2019.

[53] J. Havlicek, C. Herrojo, F. Paredes, J. Mata-Contreras and F. Martín, "Enhancing the per-unit-length data density in near-field chipless-RFID systems with sequential bit reading", *IEEE Ant. Wireless Propag. Lett.*, vol. 18, no. 1, pp. 89-92, Jan. 2019.

[54] C. Herrojo, F. Muela, J. Mata-Contreras, F. Paredes, F. Martín, "High-density microwave encoders for motion control and near-field chipless-RFID", *IEEE Sensors J*., vol. 19, pp. 3673-3682, May 2019.

[55] C. Herrojo, F. Paredes, and F. Martín, "Double-stub loaded microstrip line reader for very high data density microwave encoders", *IEEE Trans. Microw. Theory Techn*., vol.67, pp. 3527-3536, Sep. 2019.

[56] F. Martín, C. Herrojo, F. Paredes, and J. Mata-Contreras, *Time Domain Signature Barcodes for Chipless-RFID and Sensing Applications*, Springer, 2020.

[57] F. Paredes, C. Herrojo, F. Martin, "An approach for Synchronous Reading of Near-Field Chipless-RFID Tags", *10th IEEE International Conference on RFID Technology and Applications* (IEEE RFID-TA 2019), Pisa, Italy, 25-27 Sep. 2019.

[58] F. Falcone, T. Lopetegi, J.D. Baena, R. Marqués, F. Martín and M. Sorolla, "Effective negative-ε stop-band microstrip lines based on complementary split ring resonators", *IEEE Microw. Wireless Compon. Lett.*, vol. 14, pp. 280-282, Jun. 2004.

[59] F. Martín, *Artificial Transmission Lines for RF and Microwave Applications*, Wiley, Hoboken, NJ, 2015.

Ferran Paredes was born in Badalona (Barcelona), Spain in 1983. He received the Telecommunications Engineering Diploma (specializing in Electronics) and the Telecommunications Engineering degree from the Universitat Autònoma de Barcelona in 2004 and 2006, respectively and the PhD degree in Electronics Engineering from the same university in 2012. He was Assistant Professor from 2006 to 2008 at the Universitat Autònoma de Barcelona, where he is currently working as a Research Assistant. His research interests include metamaterial concepts, passive microwaves devices, antennas and RFID.

Cristian Herrojo was born in Barcelona, Spain, in 1983. He received the Telecommunications Technical Engineering degree in electronic systems and Telecommunications Engineering degree from the Universitat Autònoma de Barcelona in 2010 and 2012, respectively and the PhD degree in Electronics Engineering from the same university in 2018. His research interests include RF/microwave devices, Chipless-RFID and RFID technology, and Metamaterials.

Roger Escudé was born in Barcelona, Spain. He received the M.S. degree in Industrial Electronics and Automation Engineering from the Polytechnic University of Catalonia, Spain, in 2004. He is working at IMB-CNM from 2004, and from 2016 he is in charge of printed electronics laboratory. He has co-authored seven articles and holds one patent. His main interest is the research on the field of electronic hybridization mixing printed electronic technologies with others.

Eloi Ramon graduated in Telecom Engineering from the Polytechnic University of Catalonia (UPC), holds a Master in Micro- and Nanoelectronics Engineering and a PhD on inkjet printed devices and circuits from the Autonomous University of Barcelona (UAB). Since 1999, he is an Associate Professor at the Electronic Dept. (UAB) where he is teaching Telecom and CS BsC and MA. In 2014 he joined IMB-CNM as Printed Microelectronics researcher & group leader of Printed Electronics R&D line. His work is focused in the area of printed & organic devices for electronic systems, radiofrequency and biomedical applications, with large focus on the application of inkjet printing technologies for functional devices manufacturing. He has participated in more than 55 industrial and research projects, being co-author of more than 40 papers and 50 conference presentations and serving as a reviewer and scientific expert for different journals and public funding agencies.

FERRAN MARTIN (M'04-SM'08-F'12) was born in Barakaldo (Vizcaya), Spain in 1965. He received the B.S. Degree in Physics from the Universitat Autònoma de Barcelona (UAB) in 1988 and the PhD degree in 1992. From 1994 up to 2006 he was Associate Professor in Electronics at the Departament d'Enginyeria Electrònica (Universitat Autònoma de Barcelona), and since 2007 he is Full Professor of Electronics. In recent years, he has been involved in different research activities including modelling and simulation of electron devices for high frequency applications, millimeter wave and THz generation systems, and the application of electromagnetic bandgaps to microwave and millimeter wave circuits. He is now very active in the field of metamaterials and their application to the miniaturization and optimization of microwave circuits and antennas. Other topics of interest include microwave sensors and RFID systems, with special emphasis on the development of high data capacity chipless-RFID tags. He is the head of the Microwave Engineering, Metamaterials and Antennas Group (GEMMA Group) at UAB, and director of CIMITEC, a research Center on Metamaterials supported by TECNIO (Generalitat de Catalunya). He has organized several international events related to metamaterials and related topics, including Workshops at the IEEE International Microwave Symposium (years 2005 and 2007) and European Microwave Conference (2009, 2015 and 2017), and the Fifth International Congress on Advanced Electromagnetic Materials in Microwaves and Optics (Metamaterials 2011), where he acted as Chair of the Local Organizing Committee. He has acted as Guest Editor for six Special Issues on metamaterials and sensors in five International Journals. He has authored and co-authored over 600 technical conference, letter, journal papers and book chapters, he is co-author of the book on Metamaterials entitled *Metamaterials with Negative Parameters: Theory, Design and Microwave Applications* (John Wiley & Sons Inc.), author of the book *Artificial Transmission Lines for RF and Microwave Applications* (John Wiley & Sons Inc.), co-editor of the book *Balanced Microwave Filters* (Wiley/IEEE Press) and co-author of the book *Time-Domain Signature Barcodes for Chipless-RFID and Sensing Applications* (Springer). Ferran Martín has generated 19 PhDs, has filed several patents on metamaterials and has headed several Development Contracts.

Prof. Martín is a member of the IEEE Microwave Theory and Techniques Society (IEEE MTT-S). He is reviewer of the IEEE Transactions on Microwave Theory and Techniques and IEEE Microwave and Wireless Components Letters, among many other journals, and he serves as member of the Editorial Board of IET Microwaves, Antennas and Propagation, International Journal of RF and Microwave Computer-Aided Engineering, and Sensors. He is also a member of the Technical Committees of the European Microwave Conference (EuMC) and International Congress on Advanced Electromagnetic Materials in Microwaves and Optics (Metamaterials). Among his distinctions, Ferran Martín has received the 2006 Duran Farell Prize for Technological Research, he holds the *Parc de Recerca UAB – Santander* Technology Transfer Chair, and he has been the recipient of three ICREA ACADEMIA Awards (calls 2008, 2013 and 2018). He is Fellow of the IEEE and Fellow of the IET.